RSC Advances

PAPER

View Article Online
View Journal | View Issue

Cite this: *RSC Adv.*, 2015, **5**, 31282

New bipolar host materials for high performance of phosphorescent green organic light-emitting diodes†

Gyeong Heon Kim,[a] Raju Lampande,[a] Ji Hoon Kong,[a] Jung Min Lee,[a] Jang Hyuk Kwon,*[a] Jae Kyun Lee[b] and Jung Hwan Park[c]

Received 17th March 2015
Accepted 20th March 2015

DOI: 10.1039/c5ra04593b

www.rsc.org/advances

We report a series of four bipolar host materials with indenocarbozole and biphenyl pyrimidine moieties for efficient phosphorescent green organic light-emitting diodes (OLEDs). All four host materials possess excellent electro-optical properties as well as good thermal and morphological stability due to their high glass transition temperature of 129 °C and decomposition temperature of 363–401 °C. The new materials also show good triplet energy of 2.76 eV and excellent charge carrier transport properties. The fabricated OLED device with 11-[3-(2,6-diphenyl-pyrimidin-4-yl)-phenyl]-12,12-dimethyl-11,12-dihydro-11-aza-indeno[2,1-a]fluorene (mDPPICz1) as green host shows maximum current and power efficiency as high as 75.8 cd A^{-1} and 87.1 lm W^{-1} at 1000 cd m^{-2}, and an almost ideal external quantum efficiency of 21.7%.

Introduction

To achieve theoretical 100% internal quantum efficiency in organic light-emitting diodes (OLEDs), the external quantum efficiency (EQE) should be up to 20–25%.[1–5] Over the past several years, numerous classes of heavy-metal complex based phosphorescent materials have been reported that efficiently utilize triplet energy to enhance the EQE of OLED devices.[6–10] In order to produce efficient emission from phosphorescent materials, an ideal host-guest system is essential, which can transfer triplet energy from host to guest molecules. Generally, in many host-guest systems charge trapping emission is caused by large energy gaps between host and guest energy levels. In such systems, exciton self-quenching and triplet–triplet annihilation problems are unavoidable using high doping concentrations. To reduce charge trapping, the energy gap of HOMO (highest occupied molecular orbital) and LUMO (lowest unoccupied molecular orbital) between host and dopant molecules should be less than 0.2–0.3 eV.[11] In addition, charge balance is also one of the crucial parameters to enhance the efficiency of OLED devices. Better charge balance in the emissive layer not only broadens the charge recombination zone and reduces triplet–triplet annihilation but also decreases the driving voltage and enhances the operational lifetime.

Recently, several bipolar host materials for phosphorescent OLEDs have been well reported for providing a charge balance characteristics by incorporating hole and electron transporting moieties in the host molecules.[12] The reported good charge transport moieties for phosphorescent green host materials are arylamine,[13–15] carbazole[16–18] group as hole-transporting units, and fluorine,[13,20,21] oxadiazole,[14] phosphine oxide,[15,19,22] benzimidazole,[16] phenanthroimidazole,[17] triazine,[18] pyrimidine,[23,24] sulfone[25,26] as electron-transporting units. D. Ma *et al.* developed a bipolar host materials with triphenylamine and oxadiazole as hole and electron transporting moieties, which exhibits a maximum EQE of 22.7% and good charge transport characteristics for phosphorescent green device.[14] Furthermore, carbazole and benzimidazole moieties were used for improving the bipolar characteristics of green host material and demonstrated a maximum EQE, current efficiency, and power efficiency of 20.1%, 70.4 cd A^{-1}, and 63.2 lm W^{-1}, respectively.[16] Likewise, phenanthroimidazole and carbazole were utilized as the electron and hole transporting units for bipolar host materials, which, displayed a very high glass transition temperature (T_g) of 113–243 °C and decomposition temperature (T_d) of 395–417 °C. They also showed a maximum EQE of 21.0%.[17] Recently, we reported two new host materials based on the indenocarbazole unit, and they exhibit an excellent OLED device performances with good EQE value as compare to the widely used 4,4′-di(*N*-carbazolyl)biphenyl (CBP).[27] Based on these results we have developed series of host materials using indenocarbazole moiety to further enhance the OLED performances in terms of efficiency and lifetime. There are various

[a]*Department of Information Display, Kyung Hee University, Dongdaemoon-gu, Seoul, 130-701, Republic of Korea. E-mail: jhkwon@khu.ac.kr; Fax: +82-2-961-9154; Tel: +82-2-961-0948*

[b]*Center for Neuro-Medicine, Korea Institute of Science & Technology, Hwarangro 4-gil, Seongbuk-gu, Seoul 136-791, Republic of Korea*

[c]*Duksan Neolux Co., Ltd., 21-32, Ssukgol-gil, Ipjang-myeon, Seobuk-gu, Cheonan-si, Chungcheongnam-do 331-821, Republic of Korea*

† Electronic supplementary information (ESI) available. See DOI: 10.1039/c5ra04593b

other good host materials are available for phosphorescent organic electroluminescent devices; however, for the development of OLEDs synthesis of new and efficient organic host materials are still needed.

In this article, we demonstrate four new bipolar host materials, 11-[4-(2,6-diphenyl-pyrimidin-4-yl)-phenyl]-12,12-dimethyl-11,12-dihydro-11-aza-indeno[2,1-*a*]fluorene (pDPPICz1), 6-[4-(2,6-diphenyl-pyrimidin-4-yl)-phenyl]-12,12-dimethyl-6,12-dihydro-6-aza-indeno[1,2-*b*]fluorene (pDPPICz2), 11-[3-(2,6-diphenyl-pyrimidin-4-yl)-phenyl]-12,12-dimethyl-11,12-dihydro-11-aza-indeno[2,1-*a*]fluorene (mDPPICz1) and 6-[3-(2,6-diphenyl-pyrimidin-4-yl)-phenyl]-12,12-dimethyl-6,12-dihydro-6-aza-indeno [1,2-*b*]fluorene (mDPPICz2) by incorporating new indenocarbazole as the hole-transporting and biphenyl pyrimidine as the electron-transporting moiety for green phosphorescent OLEDs. Herein, the indenocarbazole and biphenyl moieties are expected to provide high hole and electron transporting property and better charge carrier stability due to longer conjugation length. We investigated the thermal, photo-physical and electrochemical properties of newly synthesized compounds. As expected the fabricated OLED devices with new host materials and $Ir(ppy)_3$ as triplet dopant show a reasonably good performance with high EQE values and longer operational stability.

Experimental section

Synthesis of 9,9-dimethyl-2-(2-nitrophenyl)-9*H*-fluorene (1)

2-(9,9-Dimethyl-9*H*-fluorene-2-yl)-4,4,5,5-tetramethyl-1,3,2-dioxaborolane (150 g, 468.41 mmol), 1-bromo-2-nitrobenzene (89.89 g, 444.99 mmol), tetrakis(triphenylphosphine) palladium(0) (27.07 g, 23.42 mmol) and potassium carbonate (2.2 M, 640 mL, 1405.24 mmol) with tetrahydrofuran (2200 mL) and water (500 mL) solvents were refluxed for 4 hours in 5 L round bottom flask. The solution was extracted with dichloromethane, and dried over anhydrous $MgSO_4$. After removal of solvent under reduced pressure, final residue was purified by column chromatography (eluent = CH_2Cl_2/hexane, 1 : 3) to get the pale yellow solid of 9,9-dimethyl-2-(2-nitrophenyl)-9*H*-fluorene (yield: 147.7 g, 84%). ^{1}H NMR ($CDCl_3$, 300 MHz) δ (ppm) 7.88–7.85 (m, 1H), 7.79–7.74 (m, 2H), 7.66–7.61 (m, 1H), 7.55–7.42 (m, 3H), 7.39–7.30 (m, 4H), 7.37–7.25 (m, 6H), 1.51 (s, 6H).

Synthesis of 12,12-dimethyl-11,12-dihydroindeno[2,1-*a*]-carbazole and 11,11-dimethyl-5,11-dihydroindeno[1,2-*b*]-carbazole (2 and 3)

A mixture of 9,9-dimethyl-2-(2-nitrophenyl)-9*H*-fluorene (56 g, 459.78 mmol) and triphenylphosphine (301.49 g, 1149.44 mmol) was dried in vacuum and filled with nitrogen gas in 5 L round bottom flask. Later, 1,2-dichlorobenzene (2200 mL) was added to dissolve the mixture and then refluxed for 12 hours in nitrogen atmosphere. After removal of solvent using distillation, the residue was divided by column chromatography (eluent = CH_2Cl_2/hexane, 1 : 7) to 12,12-dimethyl-11,12-dihydroindeno[2,1-*a*]carbazole and 11,11-dimethyl-5,11-dihydroindeno[1,2-*b*]carbazole, respectively. Finally, two residues were recrystallized with CH_2Cl_2/hexane to get white solid of 12,12-dimethyl-11,12-dihydroindeno[2,1-*a*]carbazole **(2)** and 11,11-dimethyl-5,11-dihydroindeno[1,2-*b*]carbazole **(3)**, respectively. (yield: 12,12-dimethyl-11,12-dihydroindeno[2,1-*a*]carbazole 42.5 g, 11,11-dimethyl-5,11-dihydroindeno[1,2-*b*]carbazole 37.5 g, 73%). ^{1}H NMR ($CDCl_3$, 300 MHz) δ (ppm) (12,12-dimethyl-11,12-dihydroindeno[2,1-*a*]carbazole) 8.14–8.10 (m, 3H), 7.85–7.83 (m, 1H), 7.71–7.69 (d, J = 8.0 Hz, 1H), 7.55–7.50 (m, 2H), 7.48–7.29 (m, 4H), 1.73 (s, 6H) (11,11-dimethyl-5,11-dihydroindeno[1,2-*b*]carbazole) 8.11–8.06 (m, 2H), 7.75–7.70 (m, 1H), 7.67 (s, 1H), 7.49–7.44 (m, 1H), 7.40–7.32 (m, 5H), 7.26–7.22 (m, 1H), 1.60 (s, 6H). ^{13}C NMR ($CDCl_3$, 500 MHz) δ (ppm) 153.3, 140.3, 140.1, 137.4, 135.3, 134.2, 127.2, 126.8, 125.7, 123.9, 123.5, 122.2, 120.3, 120.0, 119.8, 117.4, 112.3, 110.7, 46.7, 25.7.

Synthesis of 11-(4-bromophenyl)-12,12-dimethyl-11,12-dihydroindeno[2,1-*a*]carbazole (4)

A mixture of 12,12-dimethyl-11,12-dihydroindeno[2,1-*a*]carbazole (2, 30 g, 105.87 mmol), 1-bromo-4-iodobenzene (89.85 g, 317.61 mmol), copper powder (7.40 g, 116.46 mmol), potassium carbonate (14.63 g, 105.87 mmol) and 18-crown-6 (2.80 g, 10.59 mmol) was refluxed for 24 hours in 2 L round bottom flask at nitrogen atmosphere. After final reaction, the residue was divided by column chromatography (eluent = CH_2Cl_2/hexane, 1 : 3). Finally, the residue was recrystallized using CH_2Cl_2/hexane. (yield: 31.5 g, 68%). ^{1}H NMR ($CDCl_3$, 300 MHz) δ (ppm) 8.19–8.17 (d, J = 8.1 Hz, 1H), 8.13–8.10 (d, J = 7.2 Hz, 1H), 7.96–7.93 (d, J = 8.4 Hz, 1H), 7.80–7.73 (m, 3H), 7.43–7.40 (d, J = 8.4 Hz, 1H), 7.37–7.25 (m, 6H), 6.81–6.78 (d, J = 7.2 Hz, 1H), 1.19 (s, 6H). ^{13}C NMR ($CDCl_3$, 500 MHz) δ (ppm) 154.4, 144.44, 144.42, 139.5, 139.3, 138.9, 133.2, 133.0, 132.9, 127.0, 126.9, 125.9, 125.2, 123.8, 122.0, 120.4, 119.7, 119.5, 119.4, 113.2, 110.7, 110.6, 48.0, 26.5.

Synthesis of 5-(4-bromophenyl)-11,11-dimethyl-5,11-dihydroindeno[1,2-*b*]carbazole (5)

A mixture of 11,11-dimethyl-5,11-dihydroindeno[1,2-*b*]carbazole (3, 3 g, 17.64 mmol), 1-bromo-4-iodobenzene (15 g, 52.92 mmol), copper powder (1.23 g, 19.40 mmol), potassium carbonate (2.44 g, 17.64 mmol) and 18-crown-6 (0.46 g, 1.76 mmol) was refluxed for 24 hours in 500 mL round bottom flask at nitrogen atmosphere. After reaction, the residue was divided by column chromatography (eluent = CH_2Cl_2/hexane, 1 : 3) and recrystallized using CH_2Cl_2/hexane to get white solid. (yields: 3.0 g, 65%). ^{1}H NMR ($CDCl_3$, 300 MHz) δ (ppm) 8.17–8.14 (m, 2H), 8.13–8.10 (d, J = 8.6 Hz, 1H), 7.79–7.76 (d, J = 8.8 Hz, 1H), 7.74–7.71 (m, 1H), 7.66–7.65 (m, 1H), 7.53–7.46 (m, 2H), 7.40–7.25 (d, 6H), 1.62 (s, 6H). ^{13}C NMR ($CDCl_3$, 500 MHz) δ (ppm) 154.4, 146.7, 141.2, 140.7, 140.6, 139.2, 138.3, 137.0, 127.3, 127.0, 125.8, 123.7, 123.4, 123.3, 122.7, 120.2, 120.1, 119.9, 114.1, 109.5, 100.8, 100.7, 46.3, 28.0.

Synthesis of 11-(3-bromophenyl)-12,12-dimethyl-11,12-dihydroindeno[2,1-*a*]carbazole (6)

A mixture of 12,12-dimethyl-11,12-dihydroindeno[2,1-*a*]carbazole (2, 12 g, 42.35 mmol), 1,3-dibromobenzene (36.32 g, 127.04

mmol), copper powder (2.96 g, 46.58 mmol), potassium carbonate (5.85 g, 42.35 mmol) and 18-crown-6 (1.12 g, 4.23 mmol) was refluxed for 24 hours in 500 mL round bottom flask at nitrogen atmosphere. After reaction, the solution was purified by column chromatography (eluent = CH_2Cl_2/hexane, 1 : 4) and recrystallized using CH_2Cl_2/hexane to get white solid. (yields: 11.13 g, 60%). ^{1}H NMR ($CDCl_3$, 300 MHz) δ (ppm) 8.20–8.17 (d, J = 7.9 Hz, 1H), 8.14–8.11 (m, 1H), 7.81–7.74 (m, 3H), 7.69–7.68 (m, 1H), 7.54–7.46 (m, 2H), 7.38–7.25 (m, 5H), 6.86–6.83 (m, 1H), 1.20 (s, 4H), 1.17 (s, 2H). ^{13}C NMR ($CDCl_3$, 500 MHz) δ (ppm) 154.3, 144.3, 142.7, 139.5, 139.2, 135.7, 134.4, 132.4, 130.6, 129.8, 126.9, 126.8, 125.8, 125.1, 123.8, 122.7, 121.9, 120.4, 119.6, 119.4, 113.3, 110.6, 47.9, 26.3.

Synthesis of 5-(3-bromophenyl)-11,11-dimethyl-5,11-dihydroindeno[1,2-*b*]carbazole (7)

A mixture of 11,11-dimethyl-5,11-dihydroindeno[1,2-*b*]carbazole (3, 8.50 g, 30.00 mmol), 1,3-dibromobenzene (25.73 g, 89.99 mmol), copper powder (2.10 g, 33.00 mmol), potassium carbonate (4.15 g, 30.00 mmol) and 18-crown-6 (0.79 g, 3.00 mmol) was refluxed for 24 hours in 250 mL round bottom flask at nitrogen atmosphere. After reaction, the final mixture was divided by column chromatography (eluent = CH_2Cl_2/hexane, 1 : 4) and recrystallized using CH_2Cl_2/hexane to get white solid. (yields: 8.80 g, 67%) ^{1}H NMR ($CDCl_3$, 300 MHz) δ (ppm) 8.19–8.16 (m, 2H), 7.83–7.82 (m, 1H), 7.78–7.75 (m, 1H), 7.71–7.70 (m, 1H), 7.68–7.65 (m, 1H), 7.62–7.58 (m, 1H), 7.56–7.53 (d, J = 7.7 Hz, 1H), 7.51–7.48 (m, 1H), 7.43–7.41 (m, 2H), 7.36–7.30 (m, 3H), 1.64 (s, 6H). ^{13}C NMR ($CDCl_3$, 500 MHz) δ (ppm) 154.3, 146.7, 141.2, 140.6, 139.3, 138.3, 131.2, 130.6, 130.3, 127.3, 126.9, 125.9, 125.8, 125.7, 123.6, 123.3, 123.2, 122.6, 120.6, 120.0, 119.9, 114.0, 109.5, 100.7, 46.3, 27.9.

Synthesis of 12,12-dimethyl-11-(4-(4,4,5,5-tetramethyl-1,3,2-dioxaborolan-2-yl)phenyl)-11,12-dihydroindeno[2,1-*a*]carbazole (8)

A mixture of 11-(4-bromophenyl)-12,12-dimethyl-11,12-dihydroindeno[2,1-*a*]carbazole (4, 20.0 g, 45.62 mmol), 4,4,4′,4′,5,5,5′,5′-octamethyl-2,2′-bi(1,3,2-dioxaborolane) (12.74 g, 50.19 mmol), $PdCl_2$(dppf) (1.12 g, 1.37 mmol) and potassium acetate (13.43 g, 136.87 mmol) was dried and filled with nitrogen gas in 1 L round bottom flask. DMF (230 mL) was added to dissolve the mixture and then refluxed for 3 hours in nitrogen atmosphere. After reaction, the solution was extracted with ethyl acetate and dried over anhydrous $MgSO_4$. The dried solution was filtered. And finally the solution was purified with column chromatography (eluent = ethyl acetate/hexane, 1 : 3) and recrystallized using CH_2Cl_2/hexane to get white solid. (yield: 13.7 g, 62%). ^{1}H NMR ($CDCl_3$, 300 MHz) δ (ppm) 8.21–8.19 (d, J = 7.9 Hz, 1H), 8.14–8.11 (m, 1H), 8.08–8.05 (d, J = 8.3 Hz, 2H), 7.81–7.76 (m, 2H), 7.57–7.54 (d, J = 8.2 Hz, 1H), 7.37–7.25 (m, 5H), 6.80–6.78 (m, 1H), 1.45 (s, 12H), 1.18 (s, 6H). ^{13}C NMR ($CDCl_3$, 500 MHz) δ (ppm) 154.6, 144.6, 144.0, 139.6, 139.3, 135.94, 135.91, 130.6, 126.8, 126.7, 125.7, 125.1, 123.7, 121.9, 120.1, 119.5, 119.3, 119.3, 112.9, 110.8, 84.2, 48.0, 26.3, 24.9.

Synthesis of 11,11-dimethyl-5-(4-(4,4,5,5-tetramethyl-1,3,2-dioxaborolan-2-yl)phenyl)-5,11-dihydroindeno[1,2-*b*]carbazole (9)

A mixture of 5-(4-bromophenyl)-11,11-dimethyl-5,11-dihydroindeno[1,2-*b*]carbazole (5, 2.5 g, 5.70 mmol), 4,4,4′,4′,5,5,5′,5′-octamethyl-2,2′-bi(1,3,2-dioxaborolane) (1.59 g, 6.27 mmol), $PdCl_2$(dppf) (0.14 g, 0.17 mmol) and potassium acetate (1.678 g, 17.10 mmol) was dried and filled with nitrogen in 250 mL round bottom flask. DMF (30 mL) was added in the mixture and refluxed for 2 hours in nitrogen atmosphere. The final reacted mixture was extracted using ethyl acetate and dried over anhydrous $MgSO_4$. The dried solution was filtered. And the solution was purified by column chromatography (eluent = ethyl acetate/hexane, 1 : 4) and recrystallized using CH_2Cl_2/hexane to get white solid. (yields: 1.7 g, 62%). ^{1}H NMR ($CDCl_3$, 300 MHz) δ (ppm) 8.18–8.10 (m, 4H), 7.74–7.65 (m, 4H), 7.49–7.46 (m, 1H), 7.43–7.41 (m, 1H), 7.40–7.36 (m, 1H), 7.35–7.27 (m, 3H), 1.62 (s, 6H), 1.43 (s, 12H). ^{13}C NMR ($CDCl_3$, 500 MHz) δ (ppm) 154.4, 146.5, 141.2, 140.7, 140.6, 139.4, 138.2, 136.5, 127.2, 126.9, 126.3, 125.7, 123.7, 123.4, 122.7, 120.0, 119.9, 119.8, 113.9, 109.8, 101.0, 84.1, 46.3, 28.0, 24.9.

Synthesis of 12,12-dimethyl-11-(3-(4,4,5,5-tetramethyl-1,3,2-dioxaborolan-2-yl)phenyl)-11,12-dihydroindeno[2,1-*a*]carbazole (10)

A mixture of 11-(3-bromophenyl)-12,12-dimethyl-11,12-dihydroindeno[2,1-*a*]carbazole (6, 9.8 g, 22.36 mmol), 4,4,4′,4′,5,5,5′,5′-octamethyl-2,2′-bi(1,3,2-dioxaborolane) (6.25 g, 24.60 mmol), $PdCl_2$(dppf) (0.55 g, 0.67 mmol) and potassium acetate (6.58 g, 67.08 mmol) was dried and filled with nitrogen in 250 mL round bottom flask. DMF (100 mL) was added in the mixture and refluxed for 3 hours in nitrogen atmosphere. After reaction, the mixture was extracted using ethyl acetate and dried over $MgSO_4$. The dried solution was filtered. And the solution was purified by column chromatography (eluent = ethyl acetate/hexane, 1 : 4) and recrystallized using CH_2Cl_2/hexane to get white solid. (yields: 6.4 g, 59%) ^{1}H NMR ($CDCl_3$, 300 MHz) δ (ppm) 8.20–8.17 (d, J = 7.9 Hz, 1H), 8.12–8.09 (m, 1H), 8.03–8.00 (m, 1H), 7.89–7.89 (m, 1H), 7.79–7.75 (m, 2H), 7.71–7.67 (m, 1H), 7.65–7.60 (m, 1H), 7.35–7.29 (m, 2H), 7.28–7.26 (m, 2H), 7.25–7.22 (m, 1H), 6.83–6.80 (m, 1H), 1.32 (s, 7H), 1.30 (s, 5H), 1.15 (s, 3H), 1.07 (s, 3H). ^{13}C NMR ($CDCl_3$, 500 MHz) δ (ppm) 154.6, 144.7, 140.8, 139.9, 139.4, 139.3, 137.6, 135.9, 135.4, 133.7, 128.8, 126.8, 126.7, 125.6, 125.1, 123.7, 121.9, 120.0, 119.5, 119.3, 119.3, 112.8, 110.9, 84.1, 48.0, 26.3, 26.0, 25.0, 24.6.

Synthesis of 11,11-dimethyl-5-(3-(4,4,5,5-tetramethyl-1,3,2 dioxaborolan-2-yl)phenyl)-5,11-dihydroindeno[1,2-*b*]carbazole (11)

A mixture of 5-(3-bromophenyl)-11,11-dimethyl-5,11-dihydroindeno[1,2-*b*]carbazole (7, 8.0 g, 18.25 mmol), 4,4,4′,4′,5,5,5′,5′-octamethyl-2,2′-bi(1,3,2-dioxaborolane) (5.10 g, 20.07 mmol), Pd(dppf)Cl_2 (0.45 g, 0.55 mmol) and potassium acetate (5.37 g, 54.75 mmol) was dried by vacuum and filled with nitrogen in 250 mL round bottom flask. DMF (90 mL) was added to dissolve the mixture and refluxed for 3 hours in nitrogen

atmosphere. The reacted solution was extracted by ethyl acetate and dried over using $MgSO_4$. The solution was filtered. The filtered solution was purified by column chromatography (eluent = ethyl acetate/hexane, 1 : 4) and recrystallized using CH_2Cl_2/hexane to get white solid (yields: 5.4 g, 61%). ^{1}H NMR ($CDCl_3$, 300 MHz) δ (ppm) 8.18–8.15 (m, 2H), 8.05–8.04 (m, 1H), 7.98–7.97 (m, 1H), 7.96–7.95 (m, 1H), 7.72–7.69 (m, 3H), 7.67–7.64 (m, 1H), 7.49–7.46 (m, 1H), 7.40–7.34 (m, 2H), 7.32–7.26 (m, 3H), 1.63 (s, 6H), 1.37 (s, 12H). ^{13}C NMR ($CDCl_3$, 500 MHz) δ (ppm) 154.4, 146.2, 141.8, 141.2, 139.5, 138.0, 137.4, 133.9, 133.8, 130.3, 129.4, 127.1, 126.9, 125.5, 123.4, 123.2, 122.6, 119.9, 119.9, 119.7, 113.9, 109.7, 101.0, 84.1, 46.2, 28.1, 24.9.

Synthesis of 11-[4-(2,6-diphenyl-pyrimidin-4-yl)-phenyl]-12,12-dimethyl-11,12-dihydro-11-aza-indeno[2,1-*a*]fluorine (pDPPICz1)

A mixture of 12,12-dimethyl-11-(4-(4,4,5,5-tetramethyl-1,3,2-dioxaborolan-2-yl)phenyl)-11,12-dihydroindeno[2,1-*a*]carbazole (5.0 g, 10.30 mmol), 4-chloro-2,6-diphenylpyrimidine (8, 2.75 g, 10.30 mmol), tetrakis(triphenylphosphine)palladium(0) (0.36 g, 0.31 mmol) and potassium carbonate (1.5 M, 20 mL, 30.90 mmol) was dissolved in THF (60 mL) solvent in 250 mL round bottom flask, and then refluxed for 12 hours. After reaction, the solution was worked up and dried over using $MgSO_4$. Finally, the filtered residue was purified by column chromatography (eluent = CH_2Cl_2/hexane, 1 : 4) and recrystallized using CH_2Cl_2/hexane to get white solid (yields: 3.52 g, 58%). ^{1}H NMR ($CDCl_3$, 300 MHz) δ (ppm) 8.84–8.80 (m, 2H), 8.61–8.59 (m, 2H), 8.39–8.36 (m, 2H), 8.24–8.22 (m, 1H), 8.18 (s, 1H), 8.16–8.09 (m, 1H), 7.83–7.73 (m, 4H), 7.64–7.57 (m, 6H), 7.40–7.26 (m, 5H), 6.91–6.81 (m, 1H), 1.27 (s, 6H); ^{13}C NMR ($CDCl_3$, 500 MHz) δ (ppm) 165.4, 165.0, 163.6, 154.7, 144.7, 143.9, 139.8, 139.7, 139.5, 138.6, 138.2, 137.6, 136.1, 132.0, 131.2, 131.0, 129.2, 128.7, 128.6, 127.0, 126.1, 125.4, 124.1, 122.2, 120.5, 119.8, 119.6, 119.6, 113.4, 111.0, 110.6, 48.3, 26.7. Found: C, 87.8; H, 5.3; N, 7.2. Calc. for $C_{43}H_{31}N_3$: C, 87.6; H, 5.3; N, 7.1%.

Synthesis of 6-[4-(2,6-diphenyl-pyrimidin-4-yl)-phenyl]-12,12-dimethyl-6,12-dihydro-6-aza-indeno[1,2-*b*]fluorine (pDPPICz2)

A mixture of 11,11-dimethyl-5-(4-(4,4,5,5-tetramethyl-1,3,2-dioxaborolan-2-yl)phenyl)-5,11-dihydroindeno[1,2-*b*]carbazole (9, 5.0 g, 10.30 mmol), 4-chloro-2,6-diphenylpyrimidine (2.75 g, 10.30 mmol), tetrakis(triphenylphosphine)palladium(0) (0.36 g, 0.31 mmol) and potassium carbonate (1.5 M, 20 mL, 30.90 mmol) was added in THF (60 mL) solvent in 250 mL round bottom flask, and then refluxed for 6 hours. After reaction, the solution was worked up and dried over using $MgSO_4$. Finally, the filtered residue was purified by column chromatography (eluent = CH_2Cl_2/hexane, 1 : 4) and recrystallized using CH_2Cl_2/hexane (yields: 3.76 g, 65%) ^{1}H NMR ($CDCl_3$, 300 MHz) δ (ppm) 8.62–8.30 (m, 2H), 8.62–8.57 (m, 2H), 8.40–8.37 (m, 2H), 8.23–8.21 (d, 2H), 8.15 (s, 1H), 7.89–7.85 (m, 3H), 7.80–7.77 (m, 1H), 7.66–7.44 (m, 9H), 7.44–7.34 (m, 3H), 1.67 (s, 6H); ^{13}C NMR ($CDCl_3$, 500 MHz) δ (ppm) 165.2, 164.9, 164.1, 154.6, 147.0, 141.4, 140.8, 140.5, 139.6, 138.5, 138.3, 137.6, 136.6, 131.1, 131.0, 129.2, 128.7, 127.5, 127.5, 127.2, 126.0, 124.0, 123.7, 122.9, 120.5, 120.3, 120.2, 114.3, 110.5, 110.0, 101.2, 46.5, 28.2. Found: C, 87.5; H, 5.2; N, 7.1. Calc. for $C_{43}H_{31}N_3$: C, 87.6; H, 5.3; N, 7.1%.

Synthesis of 11-[3-(2,6-diphenyl-pyrimidin-4-yl)-phenyl]-12,12-dimethyl-11,12-dihydro-11-aza-indeno[2,1-*a*]fluorine (mDPPICz1)

A mixture of 12,12-dimethyl-11-(3-(4,4,5,5-tetramethyl-1,3,2-dioxaborolan-2-yl)phenyl)-11,12-dihydroindeno[2,1-*a*]carbazole (10, 5.5 g, 11.33 mmol), 4-chloro-2,6-diphenylpyrimidine (3.02 g, 11.33 mmol), tetrakis(triphenylphosphine)palladium(0) (0.39 g, 0.34 mmol) and potassium carbonate (1.5 M, 22 mL, 33.99 mmol) was added in THF (60 mL) solvent in 250 mL round bottom flask, and then refluxed for 12 hours. After reaction, the solution was worked up and dried over using $MgSO_4$. Finally, the filtered residue was purified by column chromatography (eluent = CH_2Cl_2/hexane, 1 : 4) and recrystallized using CH_2Cl_2/hexane (yields: 4.0 g, 60%). ^{1}H NMR ($CDCl_3$, 300 MHz) δ (ppm) 8.71–8.68 (m, 2H), 8.62–8.59 (m, 1H), 8.49 (s, 1H), 8.27–8.24 (m, 3H), 8.19–8.16 (m, 1H), 8.03 (s, 1H), 7.84–7.81 (m, 3H), 7.75–7.73 (m, 1H), 7.53–7.51 (m, 6H), 7.35–7.26 (m, 5H), 6.91–6.89 (m, 1H), 1.28 (s, 3H), 1.21 (s, 3H); ^{13}C NMR ($CDCl_3$, 500 MHz) δ (ppm) 165.4, 164.9, 163.5, 154.7, 144.6, 142.1, 139.8, 139.7, 139.5, 139.4, 138.0, 137.4, 136.0, 133.6, 131.1, 131.0, 130.4, 130.3, 129.1, 128.7, 128.3, 127.5, 127.1, 127.0, 126.1, 125.3, 124.0, 122.2, 120.5, 119.9, 119.6, 113.3, 111.0, 110.4, 48.3, 26.6, 26.6. Found: C, 87.5; H, 5.2; N, 7.3. Calc. for $C_{43}H_{31}N_3$: C, 87.6; H, 5.3; N, 7.1%.

Synthesis of 6-[3-(2,6-diphenyl-pyrimidin-4-yl)-phenyl]-12,12-dimethyl-6,12-dihydro-6-aza-indeno[1,2-*b*]fluorene (mDPPICz2)

A mixture of 11,11-dimethyl-5-(3-(4,4,5,5-tetramethyl-1,3,2-dioxaborolan-2-yl)phenyl)-5,11-dihydroindeno[1,2-*b*]carbazole (11, 4.0 g, 8.24 mmol), 4-chloro-2,6-diphenylpyrimidine (2.20 g, 8.24 mmol), tetrakis(triphenylphosphine)palladium(0) (0.29 g, 0.25 mmol) and potassium carbonate (1.3 M, 19 mL, 24.72 mmol) was added in THF (60 mL) solvent in 250 mL round bottom flask, and then refluxed for 8 hours. After reaction, the solution was worked up and dried over using $MgSO_4$. Finally, the filtered residue was purified by column chromatography (eluent = CH_2Cl_2/hexane, 1 : 4) and recrystallized using CH_2Cl_2/hexane (yields: 3.1 g, 64%). ^{1}H NMR ($CDCl_3$, 300 MHz) δ (ppm) 8.72–8.70 (m, 2H), 8.54–8.54 (m, 1H), 8.39–8.37 (m, 1H), 8.27–8.26 (m, 2H), 8.19–8.17 (m, 2H), 8.02 (s, 1H), 7.83–7.76 (m, 3H), 7.72–7.70 (m, 1H), 7.52–7.44 (m, 8H), 7.41–7.38 (m, 1H), 7.32–7.25 (m, 3H), 1.62 (s, 6H); ^{13}C NMR ($CDCl_3$, 500 MHz) δ (ppm) 165.3, 164.9, 164.1, 154.6, 146.9, 141.8, 141.2, 140.1, 139.6, 139.0, 138.6, 138.1, 137.5, 131.1, 131.0, 130.8, 129.7, 129.2, 128.7, 127.5, 127.5, 127.2, 126.6, 126.5, 126.0, 123.9, 123.6, 122.9, 120.3, 120.3, 120.2, 114.3, 110.7, 109.9, 101.2, 46.6, 28.3. Found: C, 87.5; H, 5.3; N, 7.3. Calc. for $C_{43}H_{31}N_3$: C, 87.6; H, 5.3; N, 7.1%.

Material characterization

^{1}H and ^{13}C NMR spectra were recorded using Bruker Avance 400 NMR spectrometer. The differential scanning calorimetry (DSC) was performed using a TA Instruments DSC Q2000. UV-vis and photoluminescence (PL) spectra were measured using SCINCO S-4100 spectrometer and JASCO FP6500 spectrometer, respectively. All reagents and solvents were purchased from Aldrich Chemical Co. and Fluka and used as received. Cyclic voltammetry (CV) was performed using EC epsilon electrochemical analysis equipment. Platinum wire and indium tin oxide (ITO) film on glass were used as counter and working electrodes respectively. Tetrabutylammonium perchlorate (Bu_4NClO_4) was used as a supporting electrolyte. Similarly, Ag wire in 0.1 M $AgNO_3$ was used as a reference electrode. Using an internal ferrocene/ferrocenium (Fc/Fc^+) standard, the potential values were converted to the saturated calomel electrode (SCE) scale. The optical band gap was determined from the tailing edge of absorption spectra in solution state. The HOMO level was obtained from the oxidation potential of CV characteristics. The LUMO level of each material was estimated from the optical band gap and HOMO level.

Fabrication and characterization of devices

ITO (sheet resistance of 10 Ω/□) covered glass substrates were sequentially cleaned ultrasonically in acetone, isopropyl alcohol, and rinsed with deionized water followed by UV–ozone treatment for 10 min. All organic layers and metal cathode were deposited by thermal vacuum deposition technique under a vacuum pressure of $\sim 1 \times 10^{-7}$ Torr without breaking vacuum pressure. The deposition rate of 0.5 Å s^{-1} was maintained for all organic layers. Deposition rates of LiF and Al were maintained at 0.1 Å s^{-1}, 5 Å s^{-1}, respectively. Finally all devices were encapsulated using glass cover and UV curable resin inside the nitrogen filled glove box. Current density–voltage–luminance (*J–V–L*) characteristics of fabricated OLED devices were measured by using a Keithley 2635A Source Meter Unit (SMU) and Konica Minolta CS-100A. Electroluminescence (EL) spectra and Commission Internationale de l'Eclairage (CIE) 1931 color coordinate were obtained using a Konica Minolta CS-2000 spectroradiometer.

Results and discussion

Theoretical calculations

The detail molecule design concept is discussed in our previous report.[27] Herein phenyl group is inserted between indenocarbazole and biphenyl pyrimidine moieties, which are connected to their *para*- and *meta*-position by Suzuki-coupling, respectively (See Scheme 1). In order to understand the structural characteristic and geometry optimization of host materials, molecular simulations were performed using density functional theory (DFT) calculation with B3LYP (beck three parameter hybrid functional[28–30] and Lee–Yang–Parr correlation functional[31]) and 6-31G(d) basis set implemented in Gaussian 09.[32] Fig. 1 represents the molecular orbital distributions of materials in the HOMO and LUMO states. It is clearly observed that the HOMO and LUMO orbitals of pDPPICz1 and mDPPICz1 are well separated but pDPPICz2 and mDPPICz2 show small coupling between both orbitals. In particular, the HOMO orbitals are mainly situated over the indenocarbazole moiety, whereas the LUMO orbitals are localized on the biphenyl pyrimidine moiety. Such well separated HOMO and LUMO orbitals are needed for the efficient charge transport and high triplet energy.

The triplet energy of the molecules are calculated from the difference between the total energy of the molecule from singlet ground state (S_0) to triplet lowest excited state (T_1). The calculated triplet energy (T_1) values from the molecular simulations of pDPPICz1, mDPPICz1 are 2.76 eV and pDPPICz2, mDPPICz2 are 2.74 eV, respectively. The relative physical properties of the host materials are summarized in Table 1. The experimental triplet energy of newly synthesized materials is approximately 0.14–0.16 eV lower than the calculated values, but it shows the same tendency in theoretical and experimental data. The high triplet energy of 2.76 eV is assigned to the proper decoupling of HOMO and LUMO orbitals. Hence, these values are suitable to use as host materials for phosphorescent green OLED devices.

The calculated HOMO energy values of pDPPICz1, pDPPICz2, mDPPICz1 and mDPPICz2 are 5.26, 5.35, 5.23 and 5.29 eV, respectively, which is slightly deeper than the experimental values. On the other hand, the calculated LUMO values of pDPPICz1, pDPPICz2, mDPPICz1 and mDPPICz2 are 1.92, 1.79, 1.88 and 1.81 eV, respectively, which is quite higher than the experimental

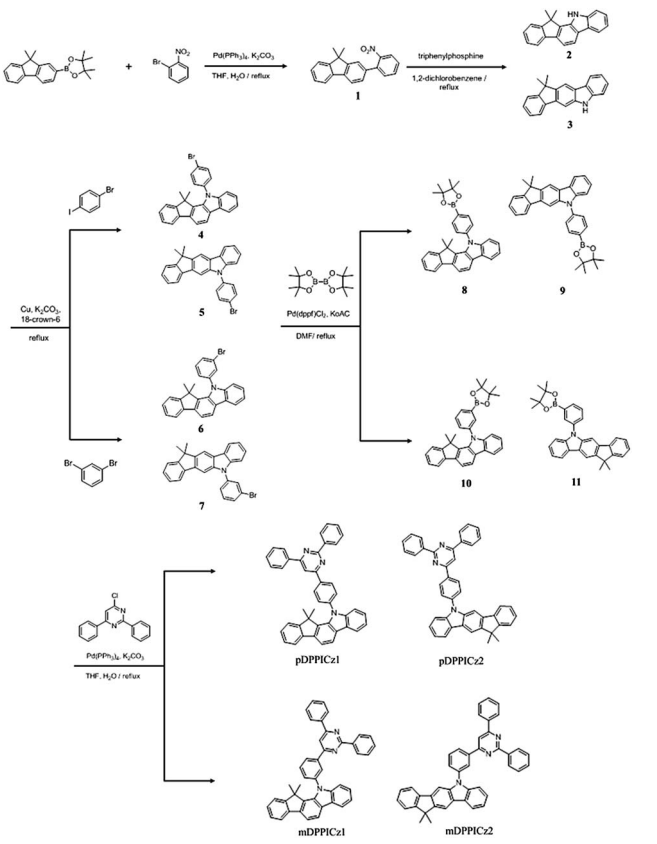

Scheme 1 Schematic route of pDPPICz1, pDPPICz2, mDPICz1 and mDPPICz2.

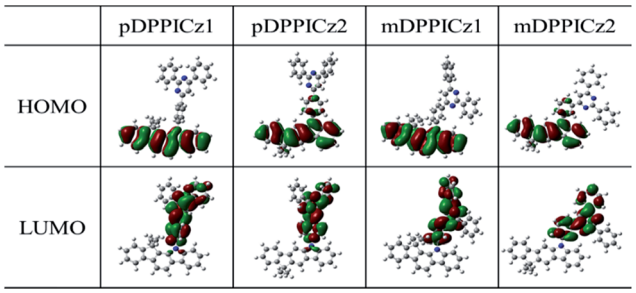

Fig. 1 Spatial distribution of the HOMO and LUMO from DFT calculation.

values. However, theoretical HOMO and LUMO values of all four materials show contrast tendency as compare to the experimental data even after the multiple runs of simulation, hence exact reason behind such tendency is unclear. The calculated band-gap values of pDPPICz1 and mDPPICz1 are 3.34 and 3.35 eV, and showing a good agreement with the experimental values. Though, this values are lower than the pDPPICz2 (3.56 eV) and mDPPICz2 (3.48 eV). The expected band gap of pDPPICz2 and mDPPICz2 could be lower than the other two materials due to their low conjugation length. Additionally, pDPPICz2 and mDPPICz2 consist of outer dimethyl group with indenocarbazole unit, which shows a smaller torsional angle between hole and electron transport moieties due to low steric hindrance results in longer conjugation length and low band gap. According to our calculations, series of newly synthesized materials have proper T_1 and appropriate HOMO, LUMO values for good phosphorescent host.

Electrical and photo-physical properties

In order to find the electrochemical properties of host materials, CV measurements were performed in acetonitrile solution using Bu_4NClO_4 10^{-4} M. The HOMO values of host materials were investigated from the onset of oxidation potential and the energy level of Fc/Fc^+ (*i.e.*, 4.80 eV). The CV characteristics of the host materials are shown in Fig. 2. The measured HOMO level of pDPPICz1, pDPPICz2, mDPPICz1 and mDPPICz2 are 5.95, 5.76, 5.76 and 5.87 eV, respectively. Similarly, the experimental LUMO energy levels of the host materials are 3.34, 3.10, 3.37 and 3.30 eV, respectively, which attained from the HOMO and optical band gap values. The optical band gap values are obtained from the tailing edge of the UV-vis absorption spectrum. The relevant electrochemical and optical data are

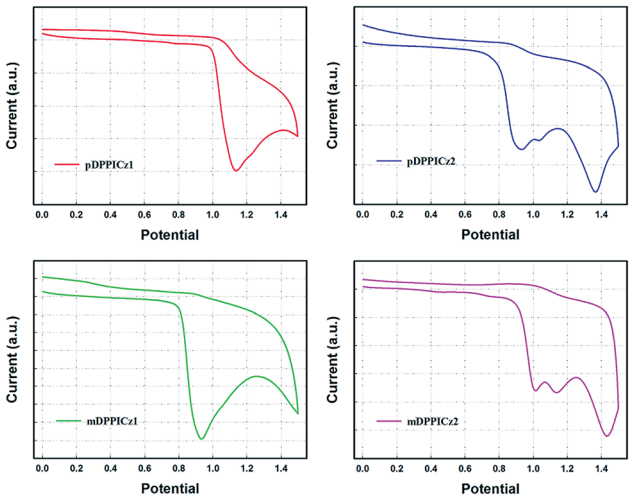

Fig. 2 CV analysis of pDPPICz1, pDPPICz2, mDPPICz1 and mDPPICz2 for oxidation potential.

summarized in Table 1. Due to relatively shorter conjugation length of pDPPICz1 and mDPPICz1 with the inner dimethyl group in indenocarbazole moiety, their energy band-gap is larger than the pDPPICz2 and mDPPICz2 with the outer dimethyl group in indenocarbazole moiety.

The UV-vis absorption and PL measurements of all four host materials were performed at room temperature in CH_2Cl_2 solution. In order to confirm the emission properties of host materials, PL measurements were performed at low temperature (77 K, see Fig. 3). The UV-visible absorption and PL characteristics of host compounds at room temperature are shown in Fig. 4. The absorption peaks are observed near 319–328 nm, which can be attributed to the π–π^* transition from indenocarbazole to biphenyl pyrimidine. The absorption peak of pDPPICz2 and mDPPICz2 is obtained at relatively longer wavelength as compare to the pDPPICz1 and mDPPICz1. On the other hand, the maximum PL peaks of pDPPICz1, pDPPICz2, mDPPICz1 and mDPPICz2 in CH_2Cl_2 solution state (1×10^{-4} M) at room temperature are observed at 449, 445, 454 and 451 nm, respectively. Although the absorption spectra of mDPPICz1 show the shortest wavelength as compare to other host materials, the PL spectra shows a red-shift result. This big Stokes shift in case of mDPPICz1 molecule could be due to the more geometrical changes as compare to other molecules from ground state to the excited state.

Table 1 Physical properties of pDPPICz1, pDPPICz2, mDPPICz1 and mDPPICz2

Host	T_g[a] [°C]	T_m[a] [°C]	T_d0.5/5.0[b] [°C]	λ_{abs}[c] [nm]	λ_{PL}[c] [nm]	E_g[d] (cal.[e]) [eV]	HOMO[f] (cal.[g]) [eV]	LUMO[h] (cal.[g]) [eV]	T_1[c,i] (cal.[g]) [eV]
pDPPICz1	NA[j]	261	358/401	319	449	3.34 (3.34)	5.95 (5.26)	2.61 (1.92)	2.62 (2.76)
pDPPICz2	NA[j]	304	315/367	328	445	3.10 (3.56)	5.76 (5.35)	2.66 (1.79)	2.58 (2.74)
mDPPICz1	NA[j]	271	325/373	319	454	3.37 (3.35)	5.76 (5.23)	2.39 (1.88)	2.62 (2.76)
mDPPICz2	129	233	327/363	326	451	3.30 (3.48)	5.87 (5.29)	2.57 (1.81)	2.58 (2.74)

[a] Measured from DSC. [b] Measured from TGA. [c] Measured in 2-methyl THF. [d] Measured by band edge of absorption spectra. [e] Values from the calculated HOMO and LUMO. [f] Determined from the onset of the oxidation potentials. [g] Values from DFT calculation B3LYP/6-31G(d). [h] Calculated from the HOMO and measured E_g. [i] Determined from peak value of low temperature PL spectra (77 K). [j] Not detected.

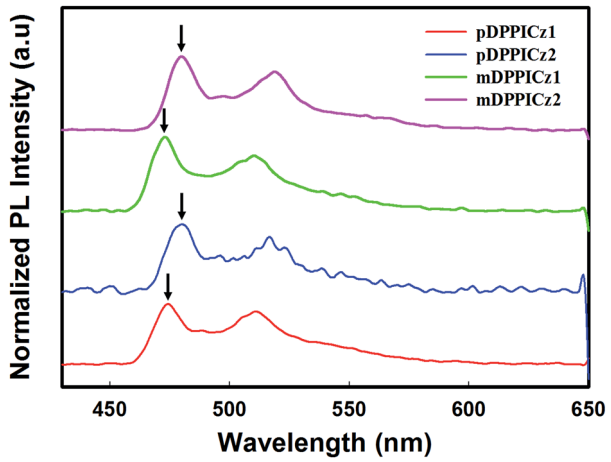

Fig. 3 Phosphorescence photoluminescence spectra in 2-methyl tetrahydrofuran solution (1×10^{-4} M) at 77 K.

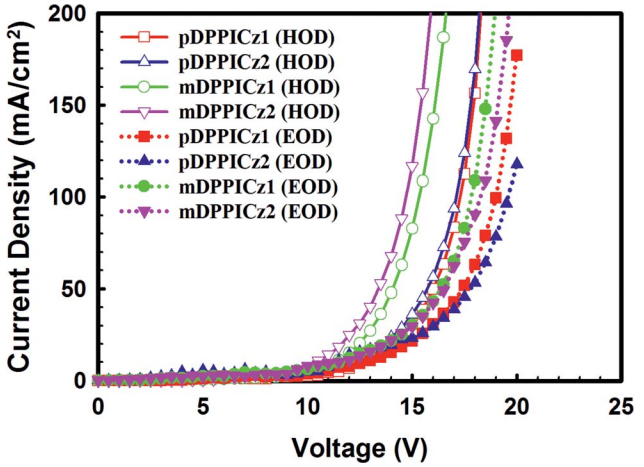

Fig. 5 *J–V* characteristics of HODs and EODs.

Thermal analysis

The ideal morphological and thermal stability of organic materials are vital for the decent operation and the better lifetime of OLED devices. Thus, thermal and morphological stabilities of new host materials were examined by using TGA and DSC. The T_d of bipolar host materials (corresponding to 5% loss) are obtained in the range of 363–401 °C, which exhibits a good thermal stability. The T_g of mDPPICz2 was observed to be 129 °C, which could be high enough to provide a morphological stability. Whereas, the noticeable T_g of other host materials was not observed. The T_g value of mDPPICz2 is higher than the commercially available CBP (62 °C).[33] We believe that these thermal properties are very well suited for the stable operation of the host materials.

Charge transport properties of host materials

To confirm the bipolar characteristics of new host materials, hole only device (HOD) and electron only device (EOD) were fabricated. The configurations of charge transport devices are as follows: HOD:ITO/di-[4-(*N*,*N*-ditolylamino)phenyl]-cyclohexane (TAPC, 80 nm)/Host (30 nm)/TAPC (40 nm)/Al (100 nm) and EOD:ITO/1,3,5-tris[(3-pyridyl)phen-3-yl]benzene (TmPyPB, 80 nm)/Host (30 nm)/TmPyPB (40 nm)/LiF (1.5 nm)/Al (100 nm). The TAPC and TmPyPB are incorporated to improve the hole and electron transport property as well as to block the injection of electrons and holes from the cathode and anode, respectively. The current density *versus* voltage (*J–V*) characteristics of HOD and EOD are shown in Fig. 5. All the four materials show higher hole current density and low electron current density. Among them mDPPICz1 shows a better hole and electron current density as compare to the other three host materials. It may be due to the better molecular packing. Interestingly, the mDPPICz2 shows higher hole current density at fix voltage (15 V) but their electron current density is lower than the mDPPICz1, which could affect the charge balance property at the emissive layer. Furthermore, pDPPICz1 and pDPPICz2 display identical charge carrier density at 15 V.

Electroluminescence properties

To evaluate the capability of series of indenocarbazole based materials as a host for green phosphorescent OLEDs, four separate devices were fabricated with the following configuration: ITO/TAPC (75 nm)/Host: 5 wt% $Ir(ppy)_3$ (15 nm)/TmPyPB (40 nm)/LiF (1 nm)/Al (100 nm). The energy level diagram of

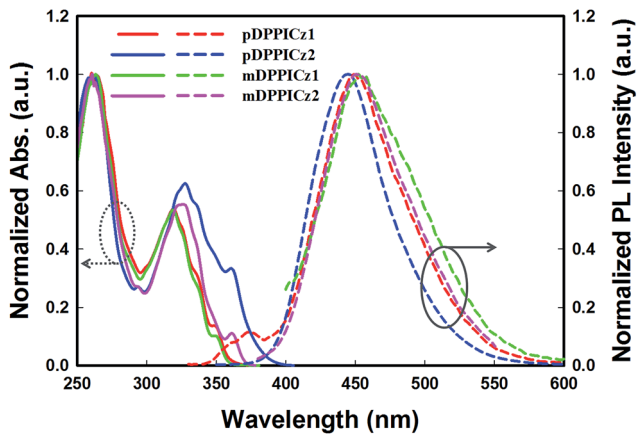

Fig. 4 UV-vis absorption and PL spectra.

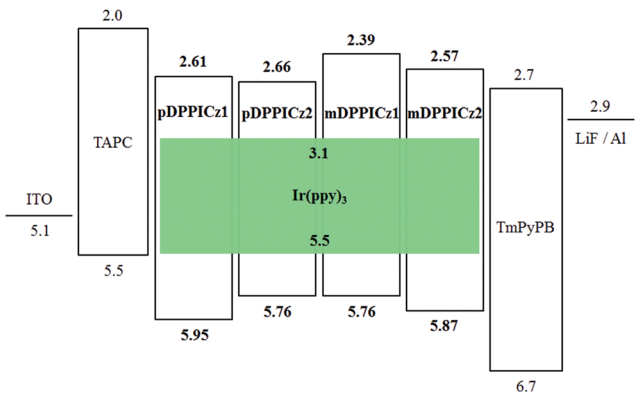

Fig. 6 Energy level diagram of fabricated green OLEDs.

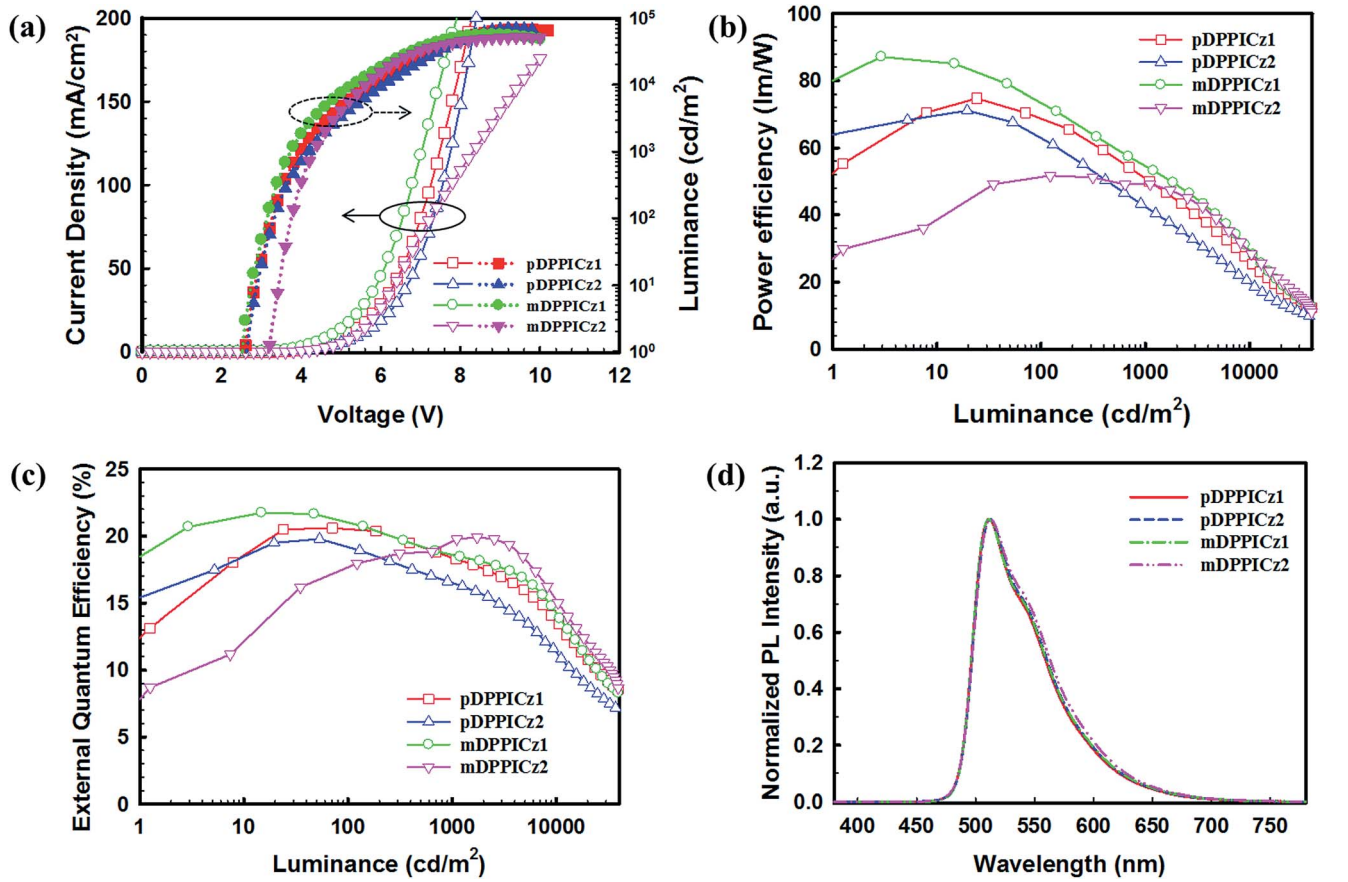

Fig. 7 Performances of bipolar host pDPPICz1, pDPPICz2, mDPPICz1 and mDPPICz2 devices. (a) *J*–*V* and *L*–*V* characteristics (b) power efficiency-luminance characteristic (c) EQE-luminance characteristics (d) EL spectra.

the fabricated green OLED device structure is shown in Fig. 6. Device A, B, C, and D are assigned to the pDPPICz1, pDPPICz2, mDPPICz1 and mDPPICz2, respectively. In these devices, ITO and Al are used as anode and cathode, respectively. The TAPC is used as a hole transport layer. However, the TmPyPB layer followed by thin LiF layer act as electron transport and injection layer, respectively. The triplet energies (T_1) of both hole and electron transport materials are high enough to block the triplet exciton quenching from the emissive layer.[34,35] $Ir(ppy)_3$ (5%) was incorporated as a green dopant in these host materials.

The *J*–*V* and *L*–*V* characteristics of the fabricated phosphorescent green OLED devices are compared in Fig. 7(a). The turn-on voltages of all four devices are in the range of 2.5–3.2 V at 1 cd m^{-2}. In particular, the Device C with mDPPICz2 shows a low turn on voltage of 2.5 V among all the studied host materials. Similarly, it also shows a low driving voltage of 3.8 V as compare to the other host materials at 1000 cd m^{-2}. We believe that, such low turn on and driving voltage values are due to the excellent bipolar and charge balance characteristics of the host materials.

The devices with pDPPICz1, pDPPICz2, mDPPICz1 and mDPPICz2 show a maximum current and power efficiency of 71.8, 68.9, 75.8 and 69.3 cd A^{-1} and 74.8, 71.1, 87.1 and 51.7 lm W^{-1} (see Fig. 7(b)), respectively. In addition the Device C shows the maximum EQE as high as 21.7%, whereas the Device A, B and D

Table 2 EL properties of pDPPICz1, pDPPICz2, mDPPICz1 and mDPPICz2 based phosphorescent green devices

Host	Turn-on voltage[a] [V]	Driving voltage[b] [V]	Max. luminance [cd m^{-2}]	Efficiency[b] (max.)			CIE 1931 (x, y)[b]
				CE[c] [cd A^{-1}]	PE[d] [lm W^{-1}]	EQE [%]	
pDPPICz1	2.7	4.0	68 090	63.6 (71.8)	50.0 (74.8)	18.3 (20.6)	(0.29, 0.63)
pDPPICz2	2.7	4.3	56 460	57.8 (68.9)	43.3 (71.1)	16.6 (19.5)	(0.30, 0.63)
mDPPICz1	2.5	3.8	56 440	64.3 (75.8)	53.2 (87.1)	18.5 (21.7)	(0.30, 0.62)
mDPPICz2	3.2	4.4	41 420	68.9 (69.3)	49.2 (51.7)	19.8 (19.9)	(0.30, 0.62)

[a] Measured at 1 cd m^{-2}. [b] measured at 1000 cd m^{-2}. [c] Current efficiency. [d] Power efficiency.

show an EQE of 20.6, 19.5, and 19.9%, respectively (see Fig. 7(c)). The EQE values of OLED device with our host materials are better than the previously reported indenofluorene (EQE: 15.8%)[36] and dihydroindenofluorene (EQE: 14.8%)[21] based host materials. The EL spectra of Device A–D are almost identical and all the devices emit green light at the emission of $Ir(ppy)_3$ (see Fig. 7(d)). The detail performances of fabricated phosphorescent green OLEDs are summarized in Table 2.

Additionally, the operational stability of fabricated OLEDs with new indenocarbazole based host materials was evaluated. The pDPPICZ1 and mDPPICz1 based devices show longer lifetime (LT_{75}) of 15 and 19 hours at initial brightness value of 1000 cd m^{-2} as compared to the widely used CBP host device. In particular, mDPPICz1 based device shows 27% longer lifetime than the pDPPICZ1. The operational lifetime of all the devices was measured until decrease in the luminance value to 75%. The operational stability data of OLEDs are shown in Fig. S1.†

Conclusion

In this paper, we have designed and synthesized a series of new bipolar green host materials, with indenocarbazole as hole and biphenyl pyrimidine as electron-transporting unit. These materials show ideal electro-optical and thermal properties for phosphorescent green OLED devices. These host materials also show proper charge balancing due to their excellent charge carrier transport properties. Fabricated phosphorescence green OLED devices show excellent maximum EQE of 21.7% as well as current efficiency, and power efficiency of 75.8 cd A^{-1}, and 87.1 lm W^{-1}, respectively.

Acknowledgements

This work was supported by the Human Resources Development program (no. 20134010200490) of the Korea Institute of Energy Technology Evaluation and Planning (KETEP) grant funded by the Korea government Ministry of Trade, Industry and Energy.

Notes and references

1 M. A. Baldo, D. F. O'Brien, Y. You, A. Shoustikov, S. Sibley, M. E. Thompson and S. R. Forrest, *Nature*, 1998, **395**, 151.
2 V. Cleave, G. Yahioglu, P. L. Barny, R. H. Friend and N. Tessler, *Adv. Mater.*, 1999, **11**, 285.
3 D. F. O'Brien, M. A. Baldo, M. E. Thompson and S. R. Forrest, *Appl. Phys. Lett.*, 1999, **74**, 442.
4 Y. Tao, C. Yang and J. Qin, *Chem. Soc. Rev.*, 2011, **40**, 2943.
5 A. Köhler, J. S. Wilson and R. H. Friend, *Adv. Mater.*, 2002, **14**, 701.
6 M. A. Baldo, M. E. Thompson and S. R. Forrest, *Nature*, 2000, **403**, 750.
7 B. Tong, Q. Mei, S. Wang, Y. Fang, Y. Meng and B. Wang, *J. Mater. Chem.*, 2008, **18**, 1636.
8 Y. Kawamura, K. Goushi, J. Brooks, J. J. Brown, H. Sasabe and C. Adachi, *Appl. Phys. Lett.*, 2005, **86**, 071104.
9 H. Xia, C. Zhang, S. Qiu, P. Lu, J. Zhang and Y. Ma, *Appl. Phys. Lett.*, 2004, **84**, 290.
10 Y. Chi and P. T. Chou, *Chem. Soc. Rev.*, 2007, **36**, 1421.
11 W. S. Jeon, T. J. Park, S. Y. Kim, R. Pode, J. Jang and J. H. Kwon, *Org. Electron.*, 2009, **10**, 240.
12 K. S. Yook and J. Y. Lee, *Adv. Mater.*, 2012, **24**, 3169.
13 H. F. Chen, T. C. Wang, W. Y. Hung, H. C. Chiu, C. Yun and K. T. Wong, *J. Mater. Chem.*, 2012, **22**, 9658.
14 S. Gong, Y. Chen, J. Luo, C. Yang, C. Zhong, J. Qin and D. Ma, *Adv. Funct. Mater.*, 2011, **21**, 1168.
15 X. K. Liu, C. J. Zheng, M. F. Lo, J. Xiao, C. S. Lee, M. K. Fung and X. H. Zhang, *Chem. Commun.*, 2014, **50**, 2027.
16 Y. M. Chen, W. Y. Hung, H. W. You, A. Chaskar, H. C. Ting, H. F. Chen, K. T. Wong and Y. H. Liu, *J. Mater. Chem.*, 2011, **21**, 14971.
17 H. Huang, Y. Wang, S. Zhuang, X. Yang, L. Wang and C. Yang, *J. Phys. Chem. C*, 2012, **116**, 19458.
18 X. K. Liu, C. J. Zheng, J. Xiao, J. Ye, C. L. Liu, S. D. Wang, W. M. Zhao and X. H. Zhang, *Phys. Chem. Chem. Phys.*, 2012, **14**, 14255.
19 J. Zhao, G. H. Xie, C. R. Yin, L. H. Xie, C. M. Han, R. F. Chen, H. Xu, M. D. Yi, Z. P. Deng, S. F. Chen, Y. Zhao, S. Y. Liu and W. Huang, *Chem. Mater.*, 2011, **23**, 5331.
20 S. Thiery, D. Tondelier, C. Declairieux, G. Seo, B. Geffroy, O. Jeannin, J. Rault-Berthelot, R. M'etivier and C. Poriel, *J. Mater. Chem. C*, 2014, **2**, 4156.
21 M. Romain, S. Thiery, A. Shirinskaya, C. Declairieux, D. Tondelier, B. Geffroy, O. Jeannin, J. Rault-Berthelot, R. M'etivier and C. Poriel, *Angew. Chem., Int. Ed.*, 2015, **54**, 1176.
22 L. Ding, S. C. Dong, Z. Q. Jiang, H. Chen and L. S. Liao, *Adv. Funct. Mater.*, 2015, **25**, 645.
23 S. Thiery, C. Declairieux, D. Tondelier, G. Seo, B. Geffroy, O. Jeannin, R. M'etivier, J. Rault-Berthelot and C. Poriel, *Tetrahedron*, 2014, **70**, 6337.
24 S. J. Su, C. Cai and J. Kido, *Chem. Mater.*, 2011, **23**, 274.
25 S. O. Jeon, T. Earmme and S. A. Jenekhe, *J. Mater. Chem. C*, 2014, **2**, 10129.
26 M. Romain, D. Tondelier, B. Geffroy, A. Shirinskaya, O. Jeannin, J. Rault-Berthelota and C. Poriel, *Chem. Commun.*, 2015, **51**, 1313.
27 G. H. Kim, R. Lampande, M. J. Park, H. W. Bae, J. H. Kong, J. H. Kwon, J. H. Park, Y. W. Park and C. E. Song, *J. Phys. Chem. C*, 2014, **118**, 28757.
28 A. D. Becke, *J. Chem. Phys.*, 1993, **98**, 1372.
29 A. D. Becke, *J. Chem. Phys.*, 1993, **98**, 5648.
30 A. D. Becke, *Phys. Rev. A*, 1988, **38**, 3098.
31 C. Lee, W. Yang and R. G. Parr, *Phys. Rev. B: Condens. Matter Mater. Phys.*, 1988, **37**, 785.
32 M. J. Frisch, G. W. Trucks, H. B. Schlegel, G. E. Scuseria, M. A. Robb, J. R. Cheeseman, G. Scalmani, V. Barone, B. Mennucci, G. A. Petersson, H. Nakatsuji, M. Caricato, X. Li, H. P. Hratchian, A. F. Izmaylov, J. Bloino, G. Zheng, J. L. Sonnenberg, M. Hada, M. Ehara, K. Toyota, R. Fukuda, J. Hasegawa, M. Ishida, T. Nakajima, Y. Honda, O. Kitao, H. Nakai, T. Vreven, J. A. J. Montgomery, J. E. Peralta, F. Ogliaro, M. Bearpark, J. J. Heyd,

E. Brothers, K. N. Kudin, V. N. Staroverov, T. Keith, R. Kobayashi, J. Normand, K. Raghavachari, A. Rendell, J. C. Burant, S. S. Iyengar, J. Tomasi, M. Cossi, N. Rega, J. M. Millam, M. Klene, J. E. Knox, J. B. Cross, V. Bakken, C. Adamo, J. Jaramillo, R. Gomperts, R. E. Stratmann, O. Yazyev, A. J. Austin, R. Cammi, C. Pomelli, J. W. Ochterski, R. L. Martin, K. Morokuma, V. G. Zakrzewski, G. A. Voth, P. Salvador, J. J. Dannenberg, S. Dapprich, A. D. Daniels, O. Farkas, J. B. Foresman, J. V. Ortiz, J. Cioslowski and D. J. Fox, *Gaussian 09, Revision B.01*, Gaussian Inc., Wallingford CT, 2010.

33 M. H. Tsai, Y. H. Hong, C. H. Chang, H. C. Su, C. C. Wu, A. Matoliukstyte, J. Simokaitiene, S. Grigalevicius, J. V. Grazulevicius and C. P. Hsu, *Adv. Mater.*, 2007, **19**, 862.

34 K. Goushi, R. Kwong, J. J. Brown, H. Sasabe and C. Adachi, *J. Appl. Phys.*, 2004, **95**, 7798.

35 S. J. Su, T. Chiba, T. Takeda and J. Kido, *Adv. Mater.*, 2008, **20**, 2125.

36 L. C. Chi, W. Y. Hung, H. C. Chiub and K. T. Wong, *Chem. Commun.*, 2009, 3892.